TOWARDS A CONCEPTUAL MATHEMATICAL TOOL LINKING PHYSICAL AND BIOLOGICAL PROCESSES FOR A REDUCTION OF GHG EMISSIONS FROM AN MB-MBR PLANT

G. MANNINA*, M. CAPODICI*, A. COSENZA*, D. DI TRAPANI*

* *Dipartimento di Ingegneria Civile, Ambientale, Aerospaziale, dei Materiali, Università degli Studi di Palermo, Palermo, Italy*

Keywords: Wastewater treatment; membrane; moving bed biofilm reactors; global warming potential

Abstract. *The current study explores the influence of the air flow rate on greenhouse gas (GHG) emissions (direct and indirect), the operational costs (OCs), the effluent quality index (EQI) and effluent fines (EF). An University Cape Town (UCT) moving bed (MB) membrane bioreactor (MBR) pilot plant has been considered as case study where the influence of the air flow rate on the biological and physical processes has been analyzed. Constitutive relationships between the air flow rate and some performance indicators (i.e., EQI, OCs, direct and indirect GHG emissions) have been identified. Results showed that the EQI increases at low flow rate likely due to the dissolved oxygen (DO) limitation in the biological processes. Direct GHGs are influenced by air flow exponentially increasing with the increase of the air flow due to the anoxic N2O contribution. Irreversible membrane fouling reduce from 98% to 85% with the increasing of the air flow rate from 0.57 m^3 h^{-1} to 2.56 m^3 h^{-1}. However, the increase of the air flow rate leads to the increase of the N_2O-N flux emitted from the MBR (from 40% to 80%). In order to establish a mathematical tool to reduce GHG emissions maintaining good effluent quality, results suggest of adopting a relationship based on a "multiple objective".*

1. Introduction

Wastewater treatment plants ($WWTP_S$) have a key role towards the environmental protection allowing to reduce the amount of pollutants discharged into the environment. During the last years huge efforts have been spent in order to improve the performance of WWTPs by employing new technologies (e.g. membrane or moving bed biofilm reactor) and control systems with the main aim to better operate WWTPs and consequently to reduce the mass of pollutants discharged into the receiving water bodies (RWBs) (Flores-Alsina et al., 2014). Therefore, in the past $WWTP_S$ had as the major target to prevent the RWB pollution. However, during the last few years, the environmental impacts associated with the wastewater treatment have been broaden and the "air" has been included as new target together with the "water" and "soil". Indeed, it has already been recognized in the international literature that wastewater treatment could result in direct emissions of greenhouse gases

(GHGs) such as carbon dioxide (CO_2), methane (CH_4) and nitrous oxide (N_2O), mainly due to the biological processes, as well as indirect emissions due to the power generation, chemicals manufacturing and sludge disposal (Fine and Hadas 2012; Flores-Alsina et al., 2014; Mannina et al., 2016a). Since the contribution of GHG produced by WWTPs has a positive trend with the growing of the population, GHGs have to be necessarily taken into account for future WWTPs design/operation (Gupta and Singh, 2012). More precisely, in order to reduce the overall GHGs emissions from wastewater treatment GHGs emissions have to be considered, in addition to effluent quality and operational costs, when comparing design alternatives or operation scenarios (Pan et al., 2011; Shahabadi et al., 2010; Guo et al., 2016). The erroneous operation of the existing WWTPs could strongly affect the amount of the GHGs discharged into the environment. Indeed, process operations exclusively aimed at the improvement of the effluent quality (in view to protect the water quality of the receiving water body) or at the reduction of the WWTP power use (to reduce the operational costs) could increase the amount of GHGs emission. Viceversa, strategies used to reduce the GHGs emissions (direct and indirect) could negatively affect the effluent quality. For example, by decreasing the aeration, WWTP energy consumption is decreased and consequently the indirect CO_2 emissions decrease as well. Nevertheless, the dissolved oxygen (DO) limitation could negatively affect the biological process leading to the worsening of the effluent quality and to the formation of N_2O (Kampschreur et al., 2009). This aspect become crucial when non-conventional advanced technologies (membrane bioreactor – MBR- or moving bed biofilm reactor -MBBR) are adopted for wastewater treatment. These technologies, especially the MBR, are recognized to be expensive in terms of both capital (mainly due to membrane costs) and operational costs (around 0.43 € m^{-3}, including all electricity fee, membrane replacement, chemical fees, but not including amortization of initial investment) (Gil et al., 2010). Further, since these technologies are characterized of being extremely robust to the hydraulic shock loads, thus always guaranteeing excellent effluent quality, their management is usually performed focusing the attention only on reducing the operational costs (Gil et al., 2010). Indeed, especially for MBR the trend is to reduce as much as possible the operational costs (e.g., reducing the power requirements by controlling the aeration for the fouling mitigation). However, as authors are aware no study has yet established the quantitative effect of reducing the power requirement (for example by reducing the aeration for fouling mitigation) in terms of GHG emissions. Is the trade-off between operational costs and effluent quality still valid in terms of GHG? In this context, the identification of the interrelationship between operational conditions and GHG emissions represents a key issue in view of reducing the GHG emissions by maintaining feasible operational costs and good effluent quality. Therefore, in this study direct and indirect GHG emissions as well as operational costs (OCs) and effluent quality index (EQI) have been evaluated for an University Cape Town (UCT) moving bed (MB) membrane biofilm reactor (MBR) pilot plant. The objectives of the study are: i. quantify the effect of the air flow variation, required for membrane fouling mitigation, on EQI, OC and GHG emission; ii. gaining insights in view of proposing a quantitative interrelationship among OCs, EQI and GHG. The results obtained from this study will help to establish the setting-up of a conceptual mathematical tool to be used to support decision-makers and plant managers to design, operate, and manage MBR WWTPs more sustainably in terms of operational costs and environmental impacts (both liquid and air emissions).

2. Materials and methods

2.1. Pilot plant and sampling campaign

An UCT-MB-MBR pilot plant was built at the Laboratory of Sanitary and Environmental Engineering of Palermo University. The pilot plant consisted of an anaerobic (volume 62 L), an anoxic (volume 102 L) and an aerobic (volume 211 L) tanks according to the UCT scheme. The pilot plant contained carriers in the anoxic and aerobic tanks with filling ratio of 15% and 40%, respectively. The solid-liquid separation phase was carried out by means of an ultrafiltration hollow fiber membrane (PURON®). The membrane module was located inside an aerated tank (MBR tank) (36 L). An oxygen depletion reactor (ODR) allowed the oxygen stripping in the mixed liquor recycled from the MBR tank to the anoxic one (Q_{RAS}). The membrane was periodically backwashed (every 9 min for a period of 1 min) by pumping, from the Clean In Place (CIP) tank a volume of permeate back through the membrane module. The extraction flow rate was set equal to 20 L h^{-1} (Q_{IN}). During the pilot plant operations, a 20 L h^{-1} flow rate (QR_1) was continuously recycled from the anoxic to the anaerobic tank. Furthermore, a 100 L h^{-1} flow rate (QR_2) of mixed liquor was pumped from the aerobic to the MBR tank. A net permeate flow rate of 20 L h^{-1} was extracted (Q_{OUT}) through the membrane module. Therefore, the recycled activated sludge (Q_{RAS}) from the MBR to the anoxic tank through the ODR tank was equal to 80 L h^{-1}. Each tank was equipped with a specific cover that enabled to capture the N_2O produced from each tank as well as from the entire pilot plant.

The pilot plant was operated at 30 days of sludge retention time (SRT) and fed with municipal wastewater mixed with a synthetic wastewater characterized by Sodium Acetate (CH_3COONa), glycerol ($C_3H_8O_3$), dipotassium hydrogen phosphate (K_2HPO_4). The UCT-MB-MBR pilot plant was started up with sludge inoculum, withdrawn from the WWTP of Palermo, to obtain an initial total suspended solid (TSS) concentration of 3,500 mg L^{-1}. After 68 days start-up phase, the experimental campaign was divided into four phases each characterized by a different MBR and aerobic air flow rates: Phase I, 0.57 m^3 h^{-1}; Phase II, 1.13 m^3 h^{-1}; Phase III, 1.70 m^3 h^{-1}; Phase IV, 2.26 m^3 h^{-1}. Each phase lasted one week and a constant air flow was superimposed.

In Table 1 the main influent and operational features are reported.

Table 1. *Main wastewater features and operational conditions*

Parameter	Unit	Value
COD	[mg L^{-1}]	589
N-NH_4	[mg L^{-1}]	78
Total phosphorus (TP)	[mg L^{-1}]	18
Permeate flux	[L m^{-2} h^{-1}]	21
Effluent flow rate	[L h^{-1}]	20
HRT	[h]	20

During the pilot plant operations, the influent wastewater, the mixed liquor inside the anaerobic, anoxic, aerobic and MBR tank and the effluent permeate have been sampled and analyzed for TSS, volatile suspended solids (VSS), total chemical oxygen demand (COD_{TOT}), supernatant COD (COD_{SUP}), ammonium nitrogen (NH_4-N), nitrite nitrogen (NO_2-N), nitrate nitrogen (NO_3-N), total nitrogen (TN), phosphate (PO_4-P), total phosphorus

(TP). All analyses have been carried out according to the Standard Methods (APHA, 2005); pH, dissolved oxygen (DO) and temperature were also monitored in each tank by using a multi-parameter probe.

Further, the liquid and gaseous samples were withdrawn from the anaerobic, anoxic, aerobic and MBR tanks and analyzed to determine the N_2O-N concentration according to Mannina et al. (2016b). Furthermore, the N_2O-N fluxes (gN_2O-N m^{-2} h^{-1}) from all the compartments were quantified by measuring the gas flow rates, Qgas (L min^{-1}) according to Mannina et al. (2016b).

2.2. Membrane fouling

Membrane fouling has been analysed by monitoring the total resistance (R_T) to membrane filtration, which is calculated according to Equation 1:

$$R_T = \frac{TMP}{\mu J} \quad (1)$$

where TMP is the transmembrane pressure (Pa), μ the permeate viscosity (Pa.s), and J the permeation flux (m s^{-1}).

RT can be defined as the sum between the intrinsic resistance of membrane (R_m) and the resistance due to membrane fouling (R_F). This latter can be fractionated according to Equation 2.

$$R_F = R_{PB} + R_{C,irr} + R_{C,rev} = R_T - R_m \quad (2)$$

where: R_{PB} is the irreversible resistance due to colloids and particles deposition into the membrane pore; $R_{C,irr}$ is the fouling resistance related to superficial cake deposition that can be only removed by physical cleanings (hydraulic/sponge scrubbing); $R_{C,rev}$ is the fouling resistance related to superficial cake deposition that can be removed by ordinary backwashing.

In order to analyse the specific fouling mechanisms the resistance in series resistances method according to Di Trapani et al. (2014) has been applied. In order to remove the removable fouling, at the beginning of each experimental phase a physical membrane cleaning was performed according to literature (Chang et al., 2001). According the in series resistances method during the physical membrane cleaning R_{PB}, $R_{C,irr}$ and $R_{C,rev}$ can be quantified (see for instance Di Trapani et al., 2014).

Furthermore, fouling rate (FR) [$m^{-1}d^{-1}$] has been evaluated according to Equation 3.

$$FR = \frac{R_{T,(t+1)} - R_{T,(t)}}{t} \quad (3)$$

Where $R_{T,(t+1)}$ and $R_{T,(t)}$ is the resistance at the time t+1 and t, respectively.

2.3. Performance indicators

Direct emissions were evaluated by adopting the total N_2O-N concentration in the liquid and gaseous samples withdrawn from each tank. More precisely, direct emissions were quantified both in terms of liquid and gaseous form. In order to quantify the total direct gaseous emission, the total gaseous mass of N_2O-N measured

was converted into mass of equivalent CO_2 per cubic meter of treated water (gCO_{2eq} m^{-3}) by adopting the global warming potential coefficient for N_2O (equal to 298 gCO_{2eq} gN_2O^{-1}) (IPCC 2007) and the volume treated wastewater per day. Similarly, the liquid direct emission was quantified by converting the mass of dissolved N_2O-N in the permeate into gCO_{2eq} m^{-3}.

To evaluate the indirect emissions, the energy required for the aeration Pw [kWh m^{-3}] and for the permeate extraction P_{eff} [kWh m^{-3}] were quantified. P_w and P_{eff} were expressed as gCO_{2eq} m^{-3} and € m^{-3} by means of two conversion factors: $\gamma_{power,GHG}$ [0.7 gCO_{2eq} kWh^{-1}] and γ_e [0.806 € kWh^{-1}], respectively (Mannina and Cosenza, 2015). Operational costs, OCs [€ m^{-3}], were calculated by adapting the cost function reported in Mannina and Cosenza (2015) (Equation 4). EF [€ m^{-3}] is the cost of the effluent fine including N_2O.

$$OC = \left(Pw + Peff\right)\cdot\gamma_e + EF \tag{4}$$

EF has been evaluated according to the Equation 5. More precisely, for each relevant pollutant (j), the effluent concentration (C_{jEFF}) has been compared with the imposed effluent limits ($C_{L,j}$) during the evaluation period (t_2-$t_{1)}$.

$$EF = \frac{1}{t_2 - t_1}\cdot\int_{t_1}^{t_2}\left[\frac{1}{Q_{IN}}\cdot\left(\sum_{j=1}^{n}\left(\begin{array}{l} Q_{OUT}\cdot\Delta\alpha_j\cdot C_j^{\,EFF} + \left(Q_{OUT}\right)\cdot \\ \left[\beta_{0,j} + \left(C_j^{\,EFF} - C_{L,j}\right)\cdot\left(\Delta\beta_j - \Delta\alpha_j\right)\right] \end{array}\right)\cdot\left(Heaviside\cdot\left(C_j^{\,EFF} - C_{L,j}\right)\right)\right)\right]\cdot dt \tag{5}$$

where Q_{IN} and Q_{OUT} are the influent and effluent flow, respectively; $\Delta\alpha_j$ is the slope of the curve EF versus C_{jEFF} when $C_{jEFF} < C_{L,j}$ (in this case, the function Heaviside =0); $\Delta\beta_j$ represents the slope of the curve EF versus C_{jEFF} when $C_{jEFF} > C_{L,j}$ (in this case, the function Heaviside =1); $\beta_{0,j}$ are the increment of the fines for the latter case.

In this study, the concentration of total COD (COD_{TOT}), total nitrogen (TN), phosphate (PO) and dissolved N_2O in the permeate coupled with gaseous N_2O. The same C_{jEFF} value according to Stare et al. (2007) is considered for each pollutant. For the N_2O a value the value of C_{jEFF} deduced from Flores-Alsina et al. (2014) is adopted. For $C_{L,j}$ the emissions limits mandated by Italian laws have been adopted. For N_2O no limits were found in literature, therefore the same limit for the PO is adopted.

The Effluent quality index, expressed as load of pollution unit (PU), EQI [kgPU d^{-1}] has also been adopted as performance indicator. The EQI represents the pollutant mass that is discharged throughout the evaluation period. In this study the EQI was evaluated modifying the equation proposed by Mannina and Cosenza (2015). Specifically, the mass of N_2O discharged (as liquid and gas) has been included by adopting a weighting factor for N_2O (both liquid and gaseous) equal to 100 (Equation 6).

$$EQI = \frac{1}{T\cdot 1000}\cdot\int_{to}^{t1}\left(\begin{array}{l} \beta_{COD}\cdot COD_{TOT} + \beta_{TN}\cdot TN + \beta_{PO}\cdot PO + \\ \beta_{N2Ogas}\cdot N_2O_{gas} + \beta_{N2O,L}\cdot N_2O_L \end{array}\right)\cdot Q_{OUT}\cdot dt \tag{6}$$

where β_{COD}, β_{TN}, β_{PO}, β_{N2Ogas} and $\beta_{N2O,L}$ are the weighting factors of the effluent COD_{TOT}, TN, PO, liquid N_2O in the permeate and gaseous N_2O. In this study the following weighting factors have been adopted (Mannina and Cosenza, 2015): β_{COD} = 1, β_{TN} = 20, β_{PO}= 50. For the N_2O on the basis of the study of Flores-Alsina et al. (2014) the value of 100 has been adopted both for β_{N2Ogas} and $\beta_{N2O,L}$.

2.4. Specific aeration demand

For each experimental phase the specific aeration demand based on membrane (SAD_m) [$m^3\ m^{-2}\ h^{-1}$] and the specific aeration demand based on permeate volume (SAD_p) [$m^3\ m^{-3}$] have been evaluated according to Equation 7 and Equation 8, respectively.

$$SAD_m = \frac{Q_{air}}{A_m} \qquad (7)$$

where J [$m\ h^{-1}$] is permeate flux and Q_p [$m^3\ h^{-1}$] is permeate flow rate; A_m and Q_{air} have the same meaning of Equation 7.

3. Results and Discussion

3.1. Direct, indirect emissions and performance indicators

Table 2 summarizes the results of the indirect and direct emissions for each experimental phase. Further data related to the performance indicators (EF, EQI and OC) are reported in Table 2.

By analyzing data reported in Table 2 it can be observed that indirect emissions are several orders of magnitude greater than the direct ones. Thus suggesting that to reduce the total global GHG emissions inside the pilot plant the power requirement has to be primarily reduced. However, particular operating conditions of the pilot plant could leads to the considerably increase of direct GHG emission. Indeed, the amount of direct GHG emitted from the pilot plant range between 0.006% and 0.6% of the total emission.

Table 2. *Direct and indirect emissions, performance indicators for each experimental phase*

Phase	Direct emission		Indirect emission	EF	EQI	OC
	gaseous	liquid				
	[g $CO_{2eq}\ m^{-3}$]		[kg $CO_{2eq}\ m^{-3}$]	[€ m^{-3}]	[kg PU d^{-1}]	[€ m^{-3}]
I	0.0015	1.30	3.88	0.57	1.05	1.51
	0.0022	1.81	4.20	0.39	0.61	1.49
II	0.0014	0.40	7.02	0.36	0.50	2.18
	0.0011	2.29	7.25	0.50	0.71	2.44
III	0.0339	55.96	9.48	0.62	0.92	2.96
	0.0178	15.43	10.09	0.23	0.39	2.88
IV	0.1702	3.86	12.06	0.20	0.06	3.13
	0.4761	4.22	11.84	0.14	0.14	2.96

Further, with the increase of the air flow rate (from the Phase I to the Phase IV) both direct and indirect GHG (expressed as kg (or g) of equivalent CO_2 per cubic meter of treated water) increased (Table 2). Direct emissions increased likely due to a twofold reason: i. high DO concentration inside the anoxic tank which promote the N_2O production (mainly in the liquid phase) during the denitrification; ii. an increase of the stripping effect of the dissolved N_2O with the increase of the air flow. During the Phase III the amount of influent ammonia (average value of 75 mg L^{-1}) was completely nitrified (average nitrification efficiency of 99%). However, due to the higher DO concentration inside the anoxic tank (0.04 mg L^{-1}), only the 25% (as average value) of the produced nitrate were denitrified. Therefore, a great amount of dissolved N_2O occurred inside the anoxic tank (0.48 mg L^{-1}).

Both EF and EQI decreased during the Phase IV mainly due to the complete nitrification and the decrease of the load of pollutant discharged into environment (Table 2). The OCs were strongly influenced by the increase of the air flow. Indeed, with the increase of the air flow the OCs value increased mainly due to the greater amount of power required for the aeration. Specifically, quadrupling the air flow from the Phase I to the Phase IV, the OC value doubled (from 1.5 € m^{-3} to 3.05 € m^{-3} for the Phase I and IV, respectively).

In the flowing sections, the interlinkage between the air flow EQI, EF, OC and the direct and indirect GHG emissions will be discussed in order to do the groundwork required for the future setting up of the conceptual mathematical model able to connect the physical and biological processes in the GHG emissions.

3.2. Specific aeration demand

Table 3 summarizes, for each experimental phase, the average SAD_m and the SAD_p values. By analysing data reported in Table 3 one may observe that with the increase of the air flow both SAD_m and SAD_p increase. Typical SADm values range between 0.2 and 1.5 m^3 m^{-2} h^{-1} while the value of SADp varies between 10 and 90 m^3 m^{-3} (Singh et al., 2006). The SAD_m and SAD_p depends on the type and operation of the MBR.

In our study the increase of SAD_m and the SAD_p is debited to the fact, especially for SAD_p, that the pilot plant is operated at constant permeate flux, therefore the permeate flow is constant even if the air flow is increased.

Table 3. Average *SADm and SADp for each for each experimental phase*

Phase	SAD_m [m^3 m^{-2} h^{-1}]	SAD_p [m^3 m^{-3}]
I	0.40	24.00
II	0.81	46.87
III	1.21	72.09
IV	1.61	93.91

3.3. Constitutive relations between the air flow rate, EQI, EF and OCs

In Figure 1 the correlations between the air flow and EQI (a), EF (b) and OC (c) are shown. As reported in Figure 1a, by increasing the air flow rate the EQI decreases, according to an exponential pattern (with a

correlation coefficient (R^2) equal to 0.61).

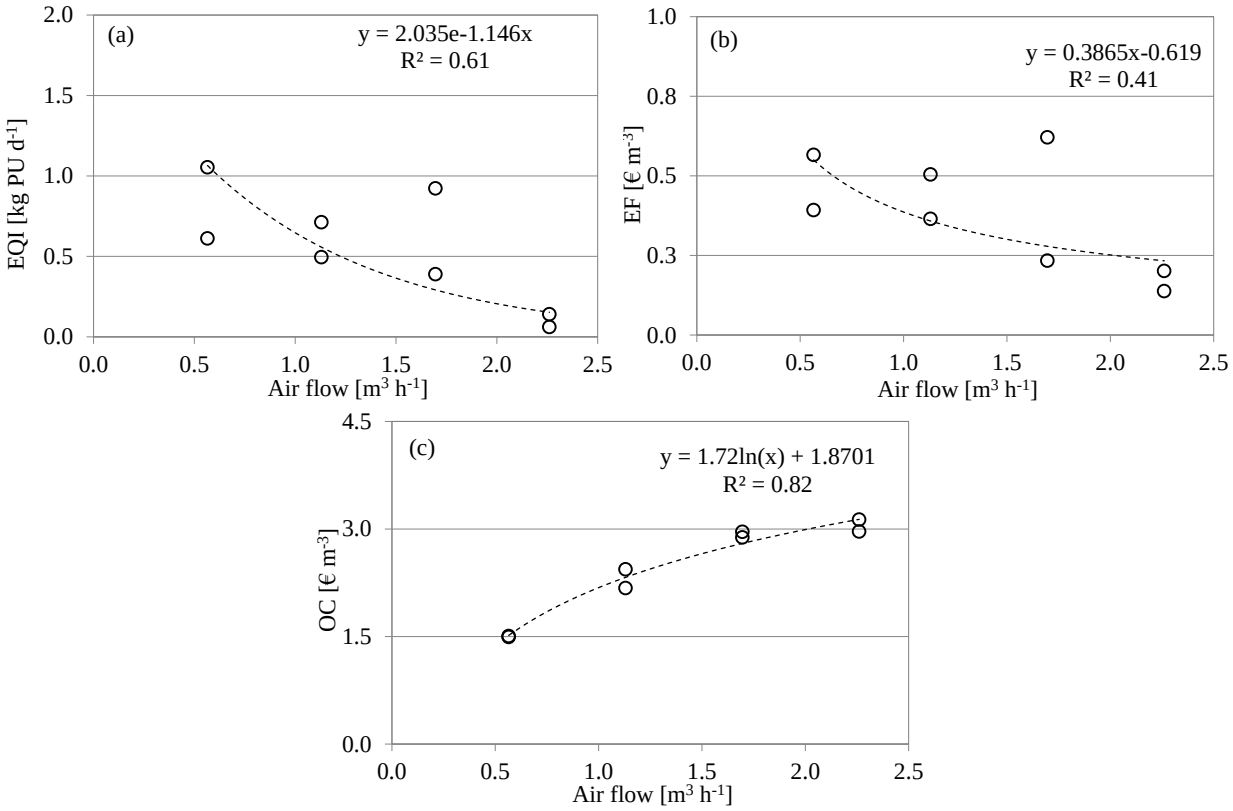

Figure 1. *Air flow versus EQI (a); EF (b) and OC (c)*

The decrease of EQI with the increase of the air flow is mainly debited to the improvement of the biological processes (carbon removal and ammonia oxidation) with the increase of the DO inside the aerated tanks and to the decrease of N_2O produced during the nitrification. Indeed, as suggested by literature, during the oxygen limiting conditions, autotrophic ammonia oxidizers use nitrite as the terminal electron acceptor to save oxygen for the oxygenation reaction of ammonia to hydroxylamine thus contributing to the N_2O production during nitrification (Kampschreur et al., 2009). However, important to precise is that high aeration may also lead to an increased amount of DO recycled in the denitrification tank which also may lead to the growth of N_2O emissions during denitrification (Kampschreur et al., 2009). The improvement of the biological processes at high air flow leads to a reduction of the mass of pollutants discharged in the environment with a consequent decrease of the fines to be payed decrease (Figure 1b). Therefore, in terms of both EQI and EF the highest air flow (Phase IV) represents the best operating condition. However, high air flow rate value entails the increase of the OC mainly due to the increase of the energy required for the aeration, Pw (Figure 1c). Thus, providing the maximum OC value (3 € m^{-3}) during the Phase IV (maximum air flow).

Therefore, to operate the plant at the highest air flow is advantageous in terms of effluent quality (the lowest EQI was obtained during the Phase IV). However, the OCs doubled during the Phase IV.

3.4. Constitutive relations between the air flow rate, direct and indirect GHG emissions

In Figure 2 data related to the relationship between the air flow versus, indirect (a) and direct emissions (b) are reported. By analysing Figure 2 one can observe that indirect GHG emissions are strongly influenced by the increase of the air flow rate (Figure 2a). More precisely, an exponential relationship (R^2 = 0.83) exists between the air flow and the direct GHG emissions, mainly due to the increase of the Pw.

An exponential relationship still exists between air flow and direct emissions (Figure 2b). Indeed, with the increase of air flow even the direct emissions increase (Figure 2b). As discussed above the great amount of DO introduced into the anoxic tank by means of the recycled sludge from the aerobic tank inhibits both synthesis and activity of denitrification enzymes leading to N_2O emission during denitrification (Otte et al., 1996). This latter consideration has paramount importance in terms of controlling the air flow: high aerobic DO reduce the amount of N_2O produced during nitrification; however, N_2O produced during denitrification increases.

In terms of only GHG emissions (both direct and indirect) the lowest air flow (Phase I) seems to be more adequate than the others. However, this result conflicts with the previous results (EQI and EF have the maximum value during the Phase I). Such result highlights the interlinkages between different involved phenomena. Indeed, a “multiple trade-off” is required in order to identify the best value of the air flow to mitigate GHG emissions and to reduce the EQI and OCs value.

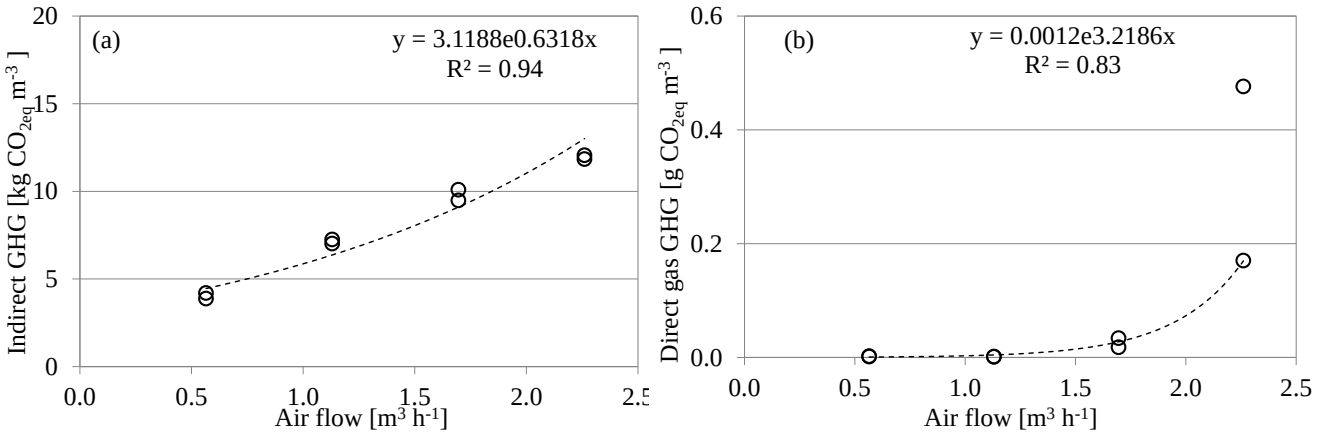

Figure 2. *Relationship between the air flow and indirect GHG emissions (a); correlation between the air flow rate direct GHG emissions (b).*

3.5. Membrane fouling and GHG emissions

Figure 3 shows the results of the application of the in series resistances method during the physical membrane cleanings operated at the beginning of the Phases I-IV (a-d) and at the end of the Phase IV (e), according to Di Trapani et al. (2014).

By analyzing Figure 3 one may observe that the variation of air flow for the fouling mitigation has strongly influenced the nature of membrane fouling. Indeed, from the Phase I (Figure 3a) to the end of the Phase IV (Figure 3d) a substantial increasing of the amount of the cake that can be removed by means of the backwashing ($R_{C,rev}$) occurred (from 1.61% to 15.21%). This result can be likely debited to the scouring effect of the high air flow (during the Phase IV) that makes the cake layer less compact thus enabling the detachment

during the backwashing. Therefore, since the minimum $R_{C,irr}$ (84.79%) value was obtained by adopting the highest air flow (Phase IV) the operating conditions related to the Phase IV represent the best way to manage the pilot plant in view of reducing membrane fouling. However, a detailed analysis of the role of high air flow (for fouling mitigation) on the GHG emission has to be performed.

With this regards Figure 4 shows the relationships between the fouling rate (FR) and the air flow (b), the N_2O-N flux emitted from the MBR tank (b) and the N_2O-N concentration of the gas samples withdrawn from the MBR (d).

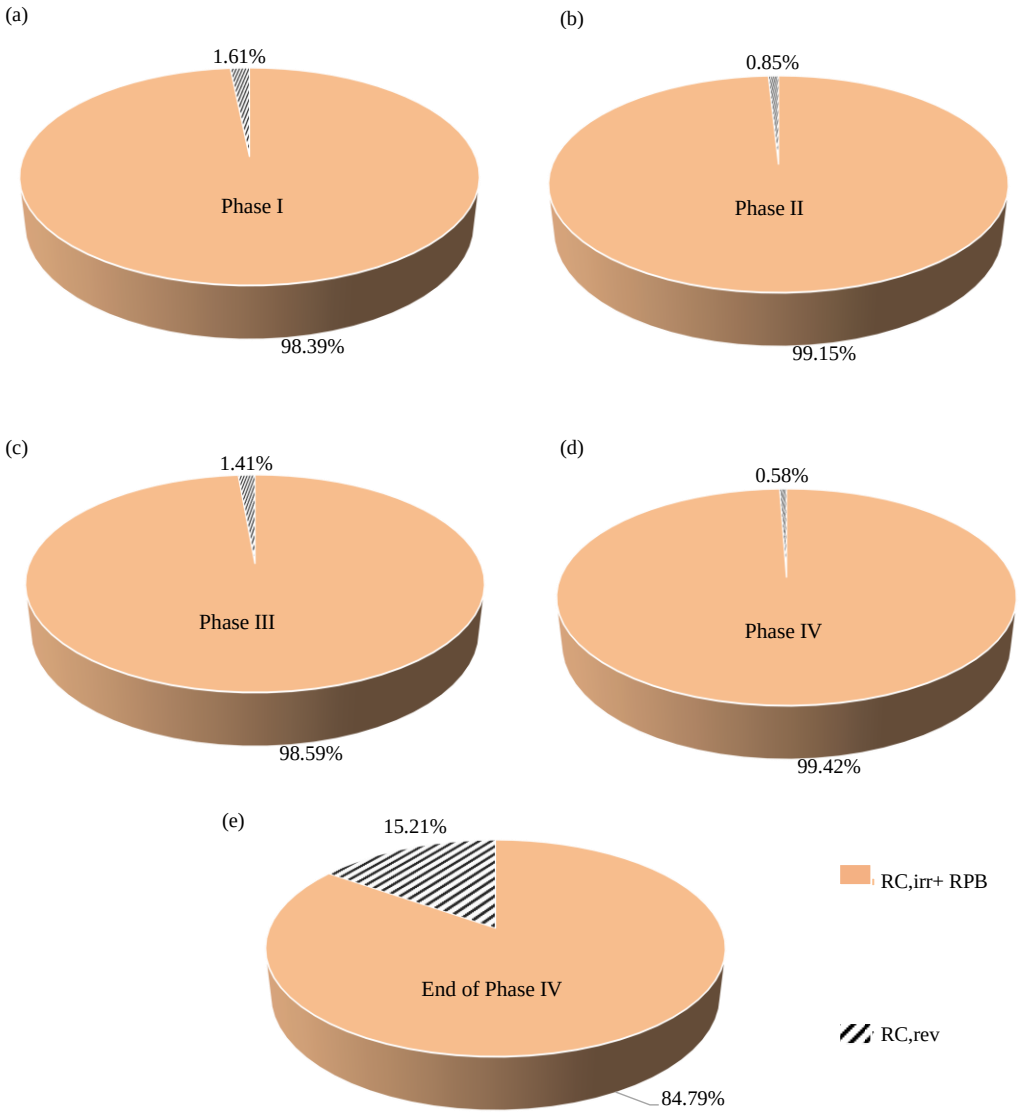

Figure 3. *Fouling fractionation according to the in series resistances method at the beginning of Phases I-IV (a-d) and at the end of the Phase IV (e.)*

Data reported in Figure 4a confirm the decrease of the membrane fouling, in terms of FR, with the increase of air flow, according to a linear relationship (R^2 = 0.88). However, the increase of the air flow negatively influence both the N_2O-N gas flux and concentration from the MBR tank. Indeed, the decrease of the FR, related to the

high air flow, leads to an increase of both the N_2O-N gas flux and gas concentration of the MBR tank (Figure 4b-c) according to an exponential relationship. This result is likely debited to the increased N_2O stripping effect at high the air flow. This result has paramount importance in terms of reducing the total GHG emission from the pilot plant because the MBR tank produce the 60% (on average) of the total N_2O flux emitted from the pilot plant.

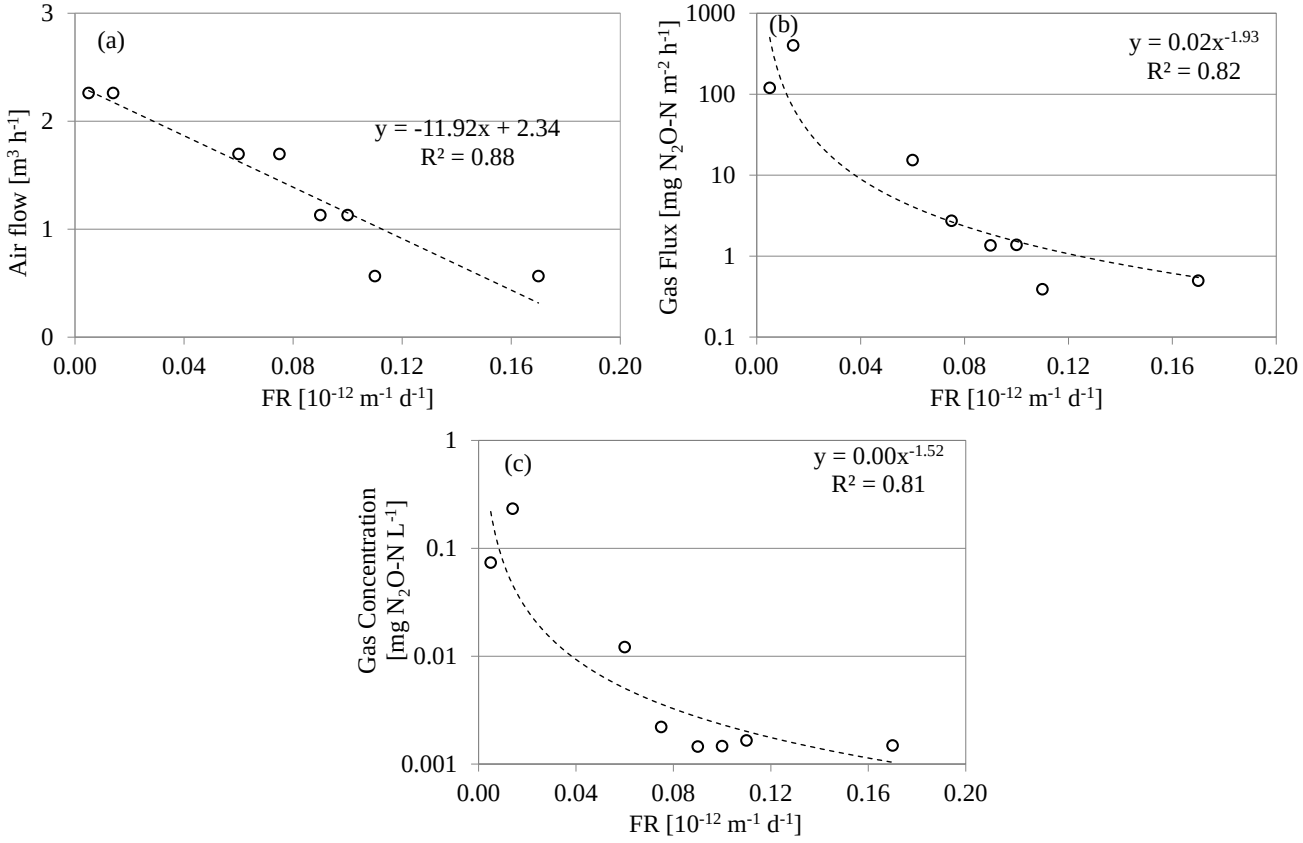

Figure 4. *Relationship between the air flow and the fouling rate (FR) (a); Relationship between N_2O-N gas flux emitted from MBR tank and FR (b); Correlation between N_2O-N gas concentration of the sample withdrawn from MBR tank and FR (c).*

4. Conclusions

To operate WWTPs with the aim to reduce direct and indirect GHGs emissions by maintaining high effluent quality is rather complicated due to the variety of processes (biological and physical) influencing their formation. The core objective of this study was to investigate the role of the air flow on the EQI, OCs, direct and indirect GHG emissions.

The main conclusions of the study are:

1) The increase of the air flow leads to a decrease of the mass of pollutants discharged in the environment (EQI) due to performance improvement of the biological processes.

2) With the increase of the air flow the OCs and the indirect GHG emissions increase due to the greater amount of power required for the aeration.

3) Direct GHG emissions increase with the increase of the air flow rate due to the great amount of N_2O produced during denitrification.

4) In terms of membrane fouling the best way to operate membrane is to adopt an high air flow (2.56 m^3 h^{-1}); however, the contribution of the MBR tank in producing N_2O increase till to the 80% of the total direct emissions.

Despite their primordial form, the results of this study will found the basis towards the establishment of a mathematical tool able to support designers/operators in view of reducing the total GHG emissions from WWTPs.

Acknowledgements

This work forms part of a research project supported by grant of the Italian Ministry of Education, University and Research (MIUR) through the Research project of national interest PRIN2012 (D.M. 28 dicembre 2012 n. 957/Ric − Prot. 2012PTZAMC) entitled “Energy consumption and GreenHouse Gas (GHG) emissions in the wastewater treatment plants: a decision support system for planning and management − http://ghgfromwwtp.unipa.it” in which the first author of this paper is the Principal Investigator.

References

[1] APHA, 2005. Standard Methods for the Examination of Water and Wastewater. APHA, AWWA and WPCF, Washington DC, USA.

[2] Chang, I.S., Bag, S.O., Lee, C.H., 2001. Effects of membrane fouling on solute rejection during membrane filtration of activated sludge. Process Biochem. 36, 855–860.

[3] Di Trapani, D., Di Bella, G., Mannina, G., Torregrossa, M., Viviani, G., 2014. Comparison between moving bed-membrane bioreactor (MB-MBR) and membrane bioreactor (MBR) systems: Influence of wastewater salinity variation. Bioresour. Technol. 162, 60–69.

[4] Fine, P., Hadas, E., 2012. Options to reduce greenhouse gas emissions during wastewater treatment for agricultural use. Sci. Total Environ. 416, 289–299.

[5] Flores-Alsina, X., Arnell,M., Amerlinck, Y., Corominas, L., Gernaey, K.V., Guo, L., et al., 2014. Balancing effluent quality, economic cost and greenhouse gas emissions during the evaluation of (plant-wide) control/operational strategies in WWTPs. Sci. Total Environ. 466–467, 616–624.

[6] Gil, J.A., Túa, L., Rueda, A., Montaño, B., Rodríguez, M., Prats, D., 2010. Monitoring and analysis of the energy cost of an MBR. Desalination 250, 997–1001.

[7] Guo, J., Fu, X., Baquero, G.A., Sobhani, R., Nolasco, D.A., Rosso, D., 2016. Trade-off between carbon emission and effluent quality of activated sludge processes under seasonal variations of wastewater temperature and mean cell retention time. Science of the Total Environment 547, 331–344.

[8] Gupta, D., Singh, S.K., 2012. Greenhouse gas emissions from wastewater treatment plants: a case study of Noida. J. Water Sustain. 2, 131–139.

[9] IPCC (2007) fourth assessment report: climate change 2007 (AR4). http://www.ipcc.ch/pdf/assessment-report/ar4/wg1/ ar4_wg1_full_report.pdf.

[10] Kampschreur, M.J., Temmink, H., Kleerebezem, R., Jetten, M.S.M., van Loosdrecht, M.C.M., 2009. Nitrous oxide emission during wastewater treatment. Water Res. 43, 4093–4103.

[11] Mannina G. and Cosenza A., 2015. Quantifying sensitivity and uncertainty analysis of a new mathematical model for the evaluation of greenhouse gas emissions from membrane bioreactors. J. Membrane Sci. 475, 80–90.

[12] Mannina, G., Ekama, G., Caniani, D., Cosenza, A., Esposito, G., Gori, R., Garrido-Baserba, M., Rosso, D., Olsson, G., 2016a. Greenhouse gases from wastewater treatment — A review of modelling tools. Science of the Total Environment 551–552, 254–270.

[13] Mannina, G., Morici, C., Cosenza, A., Di Trapani, D., Ødegaard, H. (2016b). Greenhouse gases from sequential batch membrane bioreactors: a pilot plant case study. Submitted (Under review) Bioresource Technology.

[14] Otte, S., Grobben, N.G., Robertson, L.A., Jetten, M.S.M., Kuenen, J. G., 1996. Nitrous oxide production by Alcaligenes faecalis under transient and dynamic aerobic and anaerobic conditions. Applied and Environmental Microbiology 62 (7), 2421–2426.

[15] Pan, T., Zhua, X., Ye, Y., 2011. Estimate of life-cycle greenhouse gas emissions from a vertical subsurface flow constructed wetland and conventional wastewater treatment plants: a case study in China. Ecol. Eng. 37, 248–254.

[16] Singh, R., Hoffman, E.J., Judd, S. 2006. Membranes Technology ebook. Elsevier, Amsterdam, Netherlands.

[17] Shahabadi, M.B., Yerushalmi, L., Haghighat, F., 2010. Estimation of greenhouse gas generation in wastewater treatment plants — model development and application. Chemosphere 78, 1085–1092.

[18] Stare, A., Vrecko, D., Hvala, N., Strmcnik, S., 2007. Comparison of control strategies for nitrogen removal in an activated sludge process in terms of operating costs, Water Res.41(9) 2004–2014.